

Biophysical Journal, Volume 99

Supporting Material

Squeezing protein shells: how continuum elastic models, molecular dynamics simulations and experiments coalesce at the nanoscale

Wouter H. Roos, Melissa M Gibbons, Anton Arkhipov, Charlotte Uetrecht, Norman Watts, Paul Wingfield, Alasdair C Steven, Albert Heck, Klaus Schulten, William S. Klug, and Gijs J.L. Wuite

Supplementary material

Figure S1 Histogram of HBV capsid heights with a double Gaussian fit.

The bimodal height distribution of the surface attached HBV capsids has maxima at 26.1 ± 0.4 nm ($n=55$) and 34.0 ± 0.4 nm ($n=46$). Here n is the number of particles and the uncertainty is the SEM of the fit shown in the figure. Depending on the exact binning parameters the peak values shift maximally 0.7 nm around their centre value. These peak value results correspond to the known maximum diameter of the T=3 particles without the spikes (26.2 nm) and the T=4 particles with the spikes (34.8 nm). Next to the obvious difference in size, two morphological differences between the T=3 and T=4 particles can explain the larger than expected difference in height. First, as a result of the higher curvature of the T=3 capsids, the spikes on these particles diverge more than on the T=4 particles. Therefore the glass surface and AFM tip will exert a higher perpendicular force on the spikes of the T=3 particles than of the T=4 particles. This should result in a higher degree of deformation of the spikes on T=3 particles. Second, there are ~10% less spikes per unit area for T=3 particles, which makes the collective deformation of these spikes even easier. Furthermore, the results of Böttcher *et al.* [J. Mol. Biol. Vol. 356, p812] indicate that the spikes on T=3 particles are more flexible than on T=4 capsids. Despite the differences in approaches, these results seem to correlate with our AFM data.

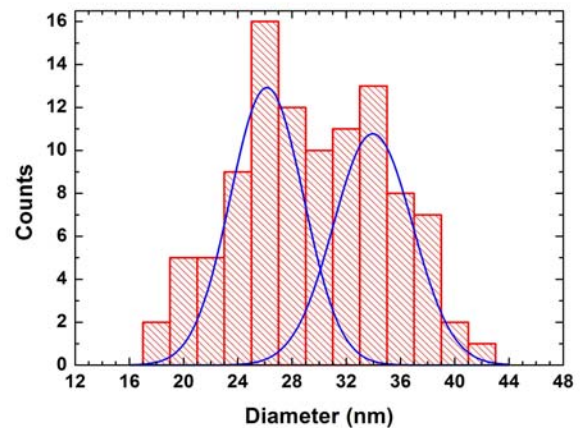
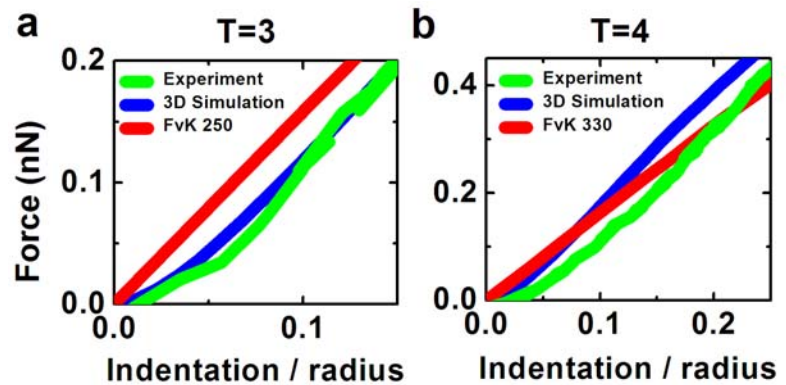


Figure S2 Zoom in on the beginning of the averaged indentation curves of Figure 1 in the main text. The difference in initial indentation behaviour can be explained considering surface features and the AFM height measurements. AFM imaging is performed at a scanning force of 0.06 - 0.1 nN and the T=3 particles appear to be imaged without spikes and the T=4 particles with spikes (see Fig. S1). The T=3 graph (a) shows an



abrupt increase in slope of the experimental curve above $F \sim 0.04$ nN, indicating the pushing aside of the spikes and subsequent indentation of the stiffer shell. For the T=4 curves (b) this increase in slope is much more gradual and continues to increase for forces significantly greater than the maximum scanning force of 0.1 nN, indicating a larger force regime over which the spikes are pushed aside and/or indented. This explains why the T=4 particles are imaged with and the T=3 particles without spikes. The 3D simulations are performed with relatively low spikes, due to a lower atom density in the spikes than in the rest of the capsid. Therefore one expects a good fit between the beginning of the T=3 experimental and 3D simulation curves and a T=4 experimental curve which is lower in the beginning than the 3D simulation curve. This is exactly what is observed. The FvK simulations are performed on thin shells without surface features and therefore no specific non-linearities are expected at the onset of indentation, nor are they observed.

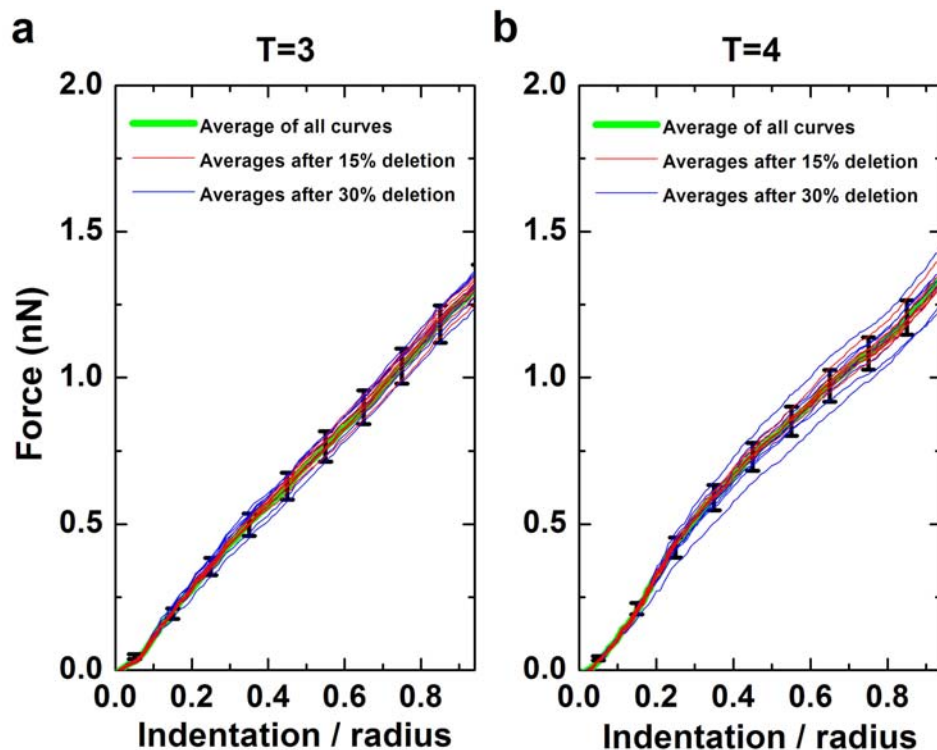


Figure S3 Testing alternative averaged curves for T=3 and T=4 particles. The thick averaged curves, in green with the error bars (SEM) in black, are the same as in Fig. 1 for T=3 (a) and T=4 (b) capsids. To test the significance of this average we randomly removed either 15% or 30% of the curves and subsequently averaged the rest, resulting in 16 new averaged curves for each capsid type. From this bootstrap-inspired procedure we see that for T=3 capsids both the 15% and 30% deletion averaged curves fall within the SEM of the total average. The 15% deletion averaged curves for T=4 also fall within the SEM of the total average, but two averaged curves of the 30% deletion set clearly fall outside this range. However, the curves that fall outside the SEM still show the general non-linear behaviour of the other curves, indicating the robustness of our total average in describing non-linear indentation behaviour.

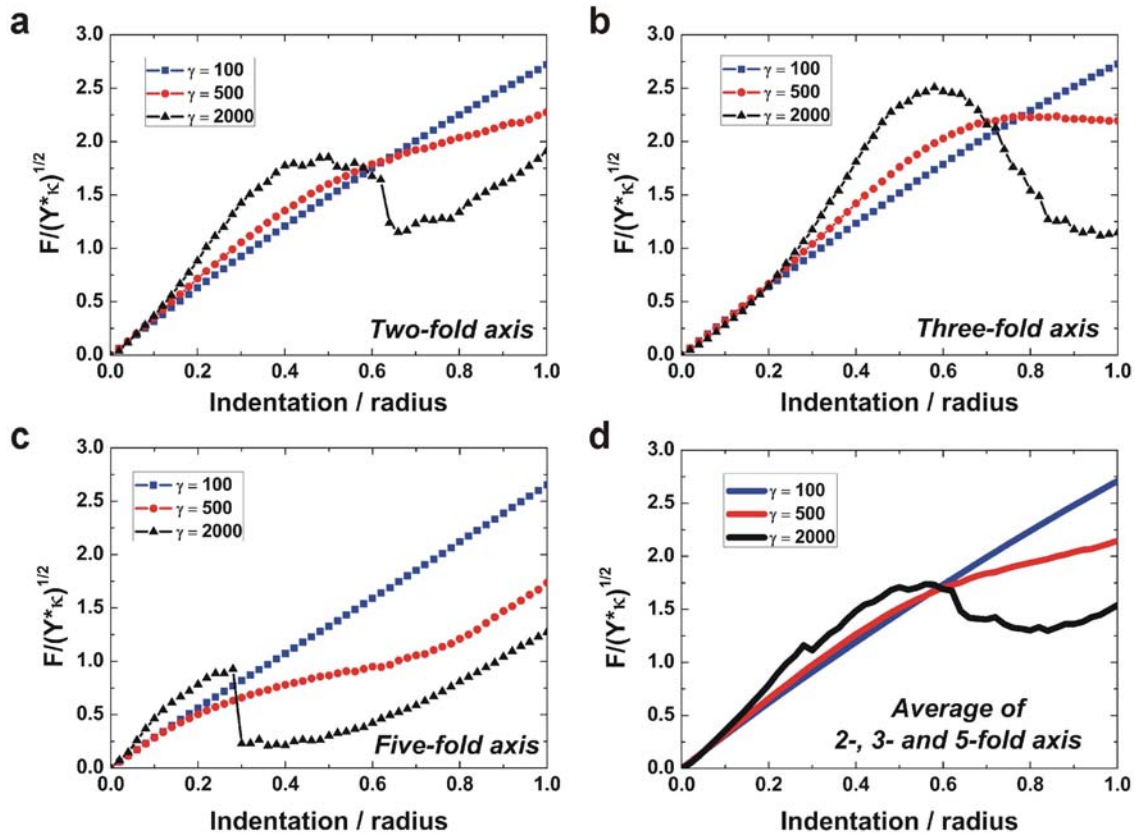


Figure S4 Thin shell simulations for various FvK numbers γ . (a) Indentation along the 2-fold symmetry axis. (b) Indentation along the 3-fold symmetry axis. (c) Indentation along the 5-fold symmetry axis. (d) Weighted averages of indentation along the 2-, 3- and 5-fold axis. Although the details are different when indentation is simulated along the various symmetry axes, the trend of increasing non-linearity with increasing FvK number is the same for all orientations.

Table S1 Number of experimental curves that were “binned” in each orientation. In the 3D line the number of experimental curves, for the respective orientations, as obtained by analysing the 3D finite element results (see Materials and Methods), are listed. The distribution of occurrence of the various symmetry sites for both the T=3 and T=4 morphologies is as expected (see main text). In the thin shell case it can be observed, by looking at the insets in figure 3, that almost no distinction can be made between the 2- and 3-fold symmetry axes. Therefore the results for these orientations are listed together. It is important to note that attempts to bin the experimental data using the thin shell simulation results produced a ratio of the number of capsids lying on the various symmetry sites that is inconsistent with the frequency of these sites occurring on an individual capsid.

	T=3 (n=31)			T=4 (n=25)		
	<i>Two-fold</i>	<i>Three-fold</i>	<i>Five-fold</i>	<i>Two-fold</i>	<i>Three-fold</i>	<i>Five-fold</i>
Expected distribution	49%	32%	19%	49%	32%	19%
#curves, 3D	55±13%	35±11%	10±6%	44±13%	40±13%	16±8%
#curves, thin shell	65±14%		35±11%	68±16%		32±11%